CO Methanation on La/Ni(111) Surface: Effect of La Electron Delocalization on Activity and Selectivity

ZHI Cuimei[1], ZHANG Riguang[2], WANG Baojun[2]
(1. College of Chemistry and bioengineering, Taiyuan University of Science and Technology, Taiyuan 030021, China)
(2. Key Laboratory of Coal Science and Technology of Ministry of Education and Shanxi Province, Taiyuan University of Technology, Taiyuan 030024, China)

Abstract: In attempting to promote the activity and selectivity of CO conversion to CH_4 and simultaneously suppress CH_3OH formation, density functional theory (DFT) calculation has been employed to insight into the reaction mechanism and the effect of the promoter La on CO conversion to CH_4 on La/Ni(111). Our results indicate that the promoter La could enrich the outer layer valence electron density of Ni, make the d-band center of La/Ni(111) upward, and thereby lead to a significant increase of the reactivity. Accordingly, the enhanced activity and selectivity to CH_4 as well as CH_3OH resistance are mainly originated from the electronic effect of the promoter La on La/Ni(111), where the synergistic effect between La and Ni plays an important role. Meanwhile, the microkinetic modeling is used to estimate the production rates of CH_4 and CH_3OH under the experimental conditions, and the result shows that $r(CH_4)$ is larger than $r(CH_3OH)$ at the same temperature, and the relative selectivity of CH_4 reaches almost as high as 100% in the temperature range of 550 to 750 K, and thereby no CH_3OH is formed when La is doped. Further, to clarify the effect of La promoter on CH_4 formation at electron level, Bader charges and the projected density of states (PDOS) have been examined for CO, HCO, COH and CH_2O, which are the key intermediates of Path1, Path2, Path3, and Path4 for CH_4 formation, respectively. The results indicate that it is electron transfer from La to Ni and the strong interaction between La and O that weaken the C—O bond and promote the cleavage of C—O bond, and thereby lead to no CH_3OH yield, which controls the selectivity to CH_4. Through analyzing the differential charge density of La atom and its surrounding Ni atoms over La/Ni(111), the result of the direction along La→Ni of charge transfer, has been shed light on furtherly. Conclusively, La/Ni(111) shows a significant increase in the activity and selectivity to CH_4 compared to Ni(111), which is mainly originated from the synergistic effect between La and Ni.

Key words: DFT; microkinetic modeling; differential charge density; synergistic effect
CLC number: O641.12+1 **Document code**: A **Article ID**: 1674-3962(2020)09-0670-11

La/Ni(111)表面 CO 甲烷化：助剂 La 对活性和选择性的影响

智翠梅[1]，章日光[2]，王宝俊[2]
(1. 太原科技大学化学与生物工程学院，山西 太原 030021)
(2. 太原理工大学 煤科学与技术教育部和山西省重点实验室，山西 太原 030024)

摘 要：针对 Ni(111)表面上因副产物 CH_3OH 形成而导致 CH_4 选择性低的问题，采用量子化学密度泛函理论(density functional theory, DFT)计算的方法，通过添加富电子的助剂 La 调节表面 Ni 原子的电子状态，增大 Ni 的 d 电子平均能以增加 La/Ni(111)表面的反应性，实现 La 与 Ni 的协同催化，从而提高 CO 甲烷化活性和 CH_4 生成选择性。同时，基于 DFT 结果，以 Microkinetic modeling 模拟实验条件下 CH_4 和 CH_3OH 的生成速率，结果表明，反应速率 r 随着温度升高而增大；在同一温度下，CH_4 生成速率 $r(CH_4)$ 远大于 CH_3OH 的生成速率 $r(CH_3OH)$，且 S_{CH_4} 在反应温度 550~750 K 内高达 100%，表明在 La/Ni(111)表面上的 CO 甲烷化过程中没有副产物 CH_3OH 的生成。究其原因，在电子水平上通过对 CH_4 形成路径 Path1、Path4、Path9 和 Path10 所对应的关键中间体 CO、

Received date: 2019-09-18 **Revised date**: 2019-12-20
Foundation item: National Natural Science Foundation of China (21736007); Research Start up Fund of Taiyuan University of Science and Technology (20182003, 20182016)
First author: ZHI Cuimei, Female, Born in 1975, Lecturer, Master tutor, Email: zhicuimei@tyust.edu.cn
Corresponding author: WANG Baojun, Male, Born in 1964, Professor, PhD supervisor, Email: wangbaojun@tyut.edu.cn
DOI: 10.7502/j.issn.1674-3962.201909017

HCO、CH_2O 和 COH 进行 Bader 电荷和 pDOS 分析，发现 C—O 键明显弱化，C—O 断键能垒显著降低，因而无 CH_3OH 生成的微观机理是 La→Ni 电子离域和 La 与 O 强相互作用而产生的“给电子诱导”效应。进一步通过 La 与邻近 Ni 原子的三维差分电荷密度分析得知，La 原子的电荷损耗是沿着“La→Ni”方向，这就给出了助剂 La 与 Ni 协同催化 CO 甲烷化并高活性高选择性地生成 CH_4 的微观解释。

关键词：密度泛函理论；microkinetic modeling；差分电荷密度；协同催化

1 Introduction

Natural gas has been considered as a promising energy source with high calorific value, while the resource reserve has been decreasing in some regions of the world. CO methanation as an available technology to manufacture synthetic natural gas (SNG) from syngas, has attained great attention from academia and industry in recent years [1, 2]. Commonly, Ni catalyst has been employed for methanation due to the high activity and low cost compared with other precious catalysts[3, 4]. However, the strongly exothermic process leads to carbon formation on the surface of nickel-based catalysts[5], besides, the catalytic activity and stability will be significantly affected with the increasing of temperature. Thus, the catalysts should be highly active and be resistant to carbon deposition.

Considerable efforts have contributed to the investigation of carbon deposition resistance[5-7], Ni(111), the greatest exposed among Ni catalyst surface, was less prone for the accumulation of C centers, irrespective of its origin, in comparison to the situation on steps, as less active for C centers formation[5]. That was a real merit the flat Ni(111) as catalytic surface should serve. Unfortunately, CO methanation of Ni(111) could be expressed mainly as a competition of $CO+3H_2 \rightarrow CH_4+H_2O$ and $CO+2H_2 \rightarrow CH_3OH$, thereby the catalytic selectivity to CH_4 will be significantly affected owing to desired product CH_3OH[7].

Many methods have been investigated for this situation, depending on La as auxiliaries[8, 9]. Doping La brought about modifications on catalytic activity, selectivity, and stability of Ni/La alloys by adjusting the electron properties for CO methanation at comparatively high temperatures with relatively less deactivation[9]. Ru/Ni/La showed much better CO methanation activity, where La was electron donors; adding La to Ru could enhance the electron density of Ru, and facilitate CO dissociation due to the back donation of the electron from Ru to CO[10]. La/Ce/Ni exhibited much higher activity for CO methanation attributing to the confinement of the interacted two promoters La and Ce for Ni nanoparticles[11]. The addition of La in the catalysts could limit the migration of the active Ni and lead to a high metal dispersion of Ni particles[11, 12] as well as good resistance to coke deposition. Additionally, the synergistic effect between La and Ni exhibited high selectivity to CH_4[13]. La/Ni alloys had been proved effective to improve the reactivity of syngas conversion to methane, resulted from the nickel lanthanum sosoloid[11-14]. Considering the above excellent performance of La/Ni catalysts, La can be a potential promoter for CO conversion to CH_4. Nevertheless, the principal reason for the observed distinctive properties by introducing La promoter was still unclear.

In this paper, using quantitative and qualitative analysis, density functional theory (DFT) calculation and microkinetic modeling were used to understand the effect of La promoter on activity and selectivity in CO methanation on La/Ni(111). To better illustrate the synergy of the promoter La and Ni, the differential charge density of the La atom and Ni atoms on La surrounding surface over La/Ni(111), as well as the d-band average energy of La/Ni(111), were investigated to prove the electron transfer occurrence of La→Ni. Specifically, to further elucidate the role of the promoter La, Bader charge analysis and projected density of states (pDOS) were performed to determine the promoting function of La promoter toward the cleavage of the C—O bond. These identified factors might offer a more comprehensive understanding of CO methanation.

2 Calculation method

2.1 Calculation models

La/Ni alloys were formed by introducing La into Ni[14]. The perovskite $LaNiO_3$ solid solution released/stored electron reversibly via La↔Ni electron delocalization; La doping was expected to enhance CO conversion and CH_4 selectivity by ordering and weakening the bond strength of CO and promoting the hydrogenation of CH_x ($x=0\sim3$), respectively. Herein, La released electrons with the C—O bond-breaking and the C—H and O—H bond-making, which was crucial for achieving high electron transfer rates[15].

A small amount of La could promote the dispersion of Ni nanoparticles, increase the content of the reduced active Ni^0, and enhance the thermal stability for CO methanation, but ex-

cess La would cover some of the Ni^0 active sites[16-18]. Besides, the aim of this work was only qualitatively reveal the role of La doping at Ni in CO methanation, and elucidate the synergistic effect between La and Ni, therefore, the structure with one La atom doping at the Ni(111) was merely considered. There is an exposure of Top, Bridge, FCC, and HCP sites on Ni(111). The site preference of La doping at Ni (111) was described based on the formation energy (E_f), as formula (1)[19]:

$$E_f = E_{La/Ni(111)} - E_{Ni(111)} - E_{La} \quad (1)$$

A negative E_f shows La doping at Ni(111) is exothermic, and the more negative E_f is, the more likely the structure is. The results of E_f were −6.81 and −6.87 eV corresponding to FCC and HCP sites; and unsurprisingly, La, originally sited at Top and Bridge sites, migrated to the nearest neighbor HCP site. According to E_f, it showed that La doping at the HCP site is favorable than other three sites, which was assigned to La/Ni (111) surface, as shown in Fig. 1

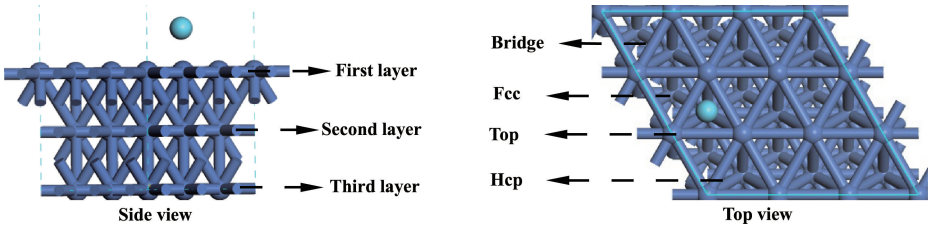

Fig. 1 The structures and preferable sites of side view and top view for La/Ni(111) surface

The La/Ni(111), a three-layer metal slab was modeled using a 3×3 supercell and vacuum regions of 15 Å, in which the bottom layer was fixed, while the two upper layers combined with the adsorbates were relaxed during optimization. The lattice constant of 3.54 Å overestimated the experimental value of 3.52 Å[20] by 0.6%.

2.2 Calculation methods

DFT calculations were carried out using the Vienna Ab Initio Simulation Package. The exchange-correlation energy functions were deduced in terms of spin-polarized Perdew-Wang (PW91) of the generalized gradient approximation (GGA)[21]. The frozen-core interaction was described by the projector-augmented wave (PAW) method[22]. Cutoff energy of 340 eV was set as the convergence of the plane-wave expansion, the Methfessel-Paxton smearing method was described with a width of 0.1 eV[23], the Monkhorst-Pack k-point mesh was set to 5×5×1 for the Brillouin zone integration.

The climbing image nudged elastic band (CI-NEB) method was employed for the minimum energy pathway[24]. The transition state (TS) was deemed converged as follows: the total energy difference was set as less than 10^{-5} eV/atom, and the residual force was set as less than 0.05 eV/Å.

The minimum adsorbate structure was obtained by the relaxation of the adsorbate and two surface layers. For the reaction on La/Ni(111), the adsorption energy (E_{ads}), the activation energy(E_a), and reaction energy (ΔE) with the zero-point-energy (ZPE) correction were defined by the equations (2), (3), and (4)[25]:

$$E_{ads} = (E_{species/slab} - E_{slab} - E_{species}) + \Delta ZPE_{ads} \quad (2)$$

$$E_a = (E_{TS} - E_{IS}) + \Delta ZPE_{barrier} \quad (3)$$

$$\Delta E = (E_{FS} - E_{IS}) + \Delta ZPE_{reaction} \quad (4)$$

ΔZPE_{ads}, $\Delta ZPE_{barrier}$, and $\Delta ZPE_{reaction}$, corrected by the ZPE, are corresponding to E_{ads}, E_a, and ΔE, respectively; which were determined by the equations (5), (6), and (7)[25].

$$\Delta ZPE_{ads} = \left(\sum_{i=1}^{vibration} \frac{hv_i}{2}\right)_{adsorbed} - \left(\sum_{i=1}^{vibrations} \frac{hv_i}{2}\right)_{gas} \quad (5)$$

$$\Delta ZPE_{barrier} = \left(\sum_{i=1}^{vibration} \frac{hv_i}{2}\right)_{TS} - \left(\sum_{i=1}^{vibrations} \frac{hv_i}{2}\right)_{IS} \quad (6)$$

$$\Delta ZPE_{reaction} = \left(\sum_{i=1}^{vibration} \frac{hv_i}{2}\right)_{FS} - \left(\sum_{i=1}^{vibrations} \frac{hv_i}{2}\right)_{IS} \quad (7)$$

where v_i represents the vibrational frequency, h is Planck's constant.

The d-band center (ε_d) of Ni(111) and La/Ni(111) were evaluated by the equation (8)[26]:

$$\varepsilon_d = \frac{\int_{-\infty}^{E_f} E\rho_d(E)\,dE}{\int_{-\infty}^{E_f} \rho_d(E)\,dE} \quad (8)$$

where $\rho_d(E)$ refers to the density of d-states at energy E.

3 Results and discussion

In this study, we will explore the role of La in La/Ni (111) toward CO methanation, which is accomplished through the comparison with the DFT results of Ni(111). Furthermore, we will describe the electron effect of the promoter

La on La/Ni(111), and explain the synergistic effect between La and Ni on CH_4 formation.

3.1 Structures and energies of all adsorbed species

The key structural parameters and E_{ads} of the stable structures of all adsorbates on La/Ni(111) were investigated in detail and summarized in Table 1. To facilitate comparison, earlier available research on Ni(111) are also tabulated. The corresponding configurations are displayed in Fig. S2 in the Supplementary material.

Table 1　Adsorption sites, adsorption energies (E_{ads}, eV), and key structural parameters of the stable configurations for the adsorbed species involved in CO methanation on La/Ni(111) surface

Species	Electronic states	E_{ads}/eV		d_{La-X}/Å
		La/Ni(111)	Ni(111)[7]	
C	triplet	−7.09 (HCP)	−6.82 (FCC), −6.82 (HCP)	$d_{La—C}$ = 2.617
H	doublet	−2.64 (HCP), −2.64 (FCC)	−2.78 (FCC), −2.77 (HCP)	$d_{La—H}$ = 2.836
O	triplet	−6.35(HCP)	−5.76 (FCC)	$d_{La—O}$ = 2.163
CO	singlet	−2.55 (HCP)	−1.90 (FCC), −1.91 (HCP)	$d_{La—O}$ = 2.457
OH	doublet	−4.33(HCP)	−3.54 (FCC)	$d_{La—O}$ = 2.952
H_2O	singlet	dissociative adsorption −5.91	−0.33 (Top)	$d_{La—O}$ = 2.902
CH	doublet	−6.37 (HCP), −6.37 (FCC)	−6.47 (FCC), −6.45 (HCP)	$d_{La—C}$ = 2.878
CH_2	singlet	−3.90(HCP), −3.90 (FCC)	−4.07 (FCC)	$d_{La—C}$ = 2.798
CH_3	doublet	−1.63 (HCP), −1.63 (FCC)	−1.94 (FCC)	$d_{La—C}$ = 2.680
CH_4	singlet	−0.07 (FCC)	−0.02 (Top)	$d_{La—C}$ = 3.489
HCO	doublet	−3.25 (FCC)	−2.35 (FCC), −2.36 (HCP)	$d_{La—O}$ = 2.329
COH	doublet	−4.44 (HCP)	−4.45 (FCC), −4.45 (HCP)	$d_{La—O}$ = 2.696
CH_2O	singlet	−1.43 (HCP)	−0.84 (FCC), −0.83 (HCP)	$d_{La—O}$ = 2.220
CH_3O	doublet	−3.51 (FCC), −3.53 (HCP)	−2.75 (FCC)	$d_{La—O}$ = 2.107
HCOH	singlet	−4.20 (HCP)	−3.91 (Bridge)	$d_{La—O}$ = 2.585
CH_2OH	doublet	−2.02 (HCP)	−1.68 (Bridge)	$d_{La—O}$ = 2.523
CH_3OH	singlet	−0.93 (Top)	−0.37 (Top)	$d_{La—O}$ = 2.582

H_2 dissociation can easily occur on La/Ni(111), it is strongly exothermic by 0.96 eV with a moderate activation barrier of 0.50 eV, and the imaginary frequency corresponding to the TS is 568 cm^{-1}, as described in Fig. S1 in the Supplementary material. The dissociated H atom adsorbs at HCP site with an E_{ads} of −2.64 eV, which are the main source of H for CO methanation. That is indeed shown to be the case in some other reports[7, 19].

The structures of C, CH, CH_2, CH_3, and CH_4 adsorbed on La/Ni(111) are much closer than those on Ni(111), and increasing order of the chemisorptive abilities are the following: CH_4<CH_3<CH_2<CH.

The geometries of the adsorptions of O, OH, and H_2O on La/Ni(111) and Ni(111) are very different, and the adsorption energies of O and OH are increase of 0.59 and 0.79 eV on La/Ni(111) compared to those on Ni(111). Interestingly, when H_2O is posited at La/Ni(111), the promoter La exhibits a strong La—O bond, leading to H_2O dissociation. OH tends to coordinate with La via O atom.

When La is introduced, CH_3O and CH_3OH adsorptions become favorable with the larger adsorption energies of −3.53 and −0.93 eV, respectively. The geometries in Fig. S1 in the Supplementary material for the adsorptions of CH_3O and CH_3OH on La/Ni(111) vary obviously, with O—La rather than O—Ni bonds, compared with the situations on Ni(111).

The adsorbed CO, HCO, CH_2O, HCOH, and CH_2OH bind to La/Ni(111) via both C and/or O atoms in a similar way to Ni(111). The difference is that O is nearing and pointing toward La, and the adsorption energies on La/Ni(111) are increased by 0.64, 0.89, 0.59, 0.29, and 0.34 eV compared to those on Ni(111), respectively. Coincidentally, the geometry and adsorption intensity of COH on La/Ni(111)

resembles that on Ni(111).

Above all, La—O bond can strengthen the adsorption of oxygenates, and the dopant La accepts electrons from the lone pair of which.

3.2 The mechanism of CO methanation on La/Ni (111) surface

The syngas on La/Ni(111) mainly gain CH_4 and CH_3OH as products. We have investigated the mechanisms consisting of elementary steps, and the main configurations for the ISs, TSs, and FSs. The potential energy diagrams are displayed in Fig. S3 and Fig. S4 in the Supplementary material, respectively. To compare E_a, ΔE, and k for steps at 550 K obtained in this work with the literature, the previous results of Ni(111) are also listed in Table 2.

Table 2 Activation barriers (E_a/eV), the reaction energies (ΔE/eV), and the rate constants $k(s^{-1})$ (T=550 K) of all possible elementary reactions involved in CO methanation on La/Ni(111) surface

Reaction		Our results				Previous results[7]		
		E_a/eV	ΔE/eV	v/cm^{-1}	k/s^{-1}	E_a/eV	ΔE/eV	v/cm^{-1}
CO→C+O	R1	1.63	1.12	56 i	8.74×10^{-2}	3.74	1.42	537 i
CO+H→HCO	R2	0.95	0.92	433 i	4.62×10^{4}	1.38	1.17	303 i
CO+H→COH	R3	2.11	1.54	1550 i	7.57×10^{-7}	1.94	0.92	1558 i
HCO→CH+O	R4	1.04	−0.11	483 i	2.17×10^{3}	1.16	−0.28	515 i
C+H→CH	R5	0.52	−0.29	953 i	7.10×10^{8}	0.92	−0.46	822 i
CH+H→CH_2	R6	0.65	0.34	697 i	2.57×10^{7}	0.74	0.34	754 i
CH_2+H→CH_3	R7	0.89	0.10	1013 i	2.86×10^{5}	0.77	−0.08	747 i
CH_3+H→CH_4	R8	0.45	−0.33	42 i	9.48×10^{9}	0.96	−0.17	1033 i
O+H→OH	R9	0.79	−0.11	1228 i	2.79×10^{6}	1.21	0.06	1204 i
HCO+H→HCOH	R10	1.47	1.16	1137 i	2.87×10^{-1}	0.92	0.34	1296 i
HCOH→CH+OH	R11	0.21	−1.43	417 i	2.06×10^{11}	0.79	−0.47	302 i
HCOH+H→CH_2OH	R12	0.65	0.07	948 i	1.44×10^{7}	0.87	0.25	841 i
CH_2OH→CH_2+OH	R13	0.40	−1.20	330 i	4.12×10^{9}	0.85	−0.38	398 i
CH_2OH+H→CH_3OH	R14	0.93	−0.21	980 i	6.11×10^{4}	0.72	−0.27	941 i
HCO+H→CH_2O	R15	0.95	0.69	832 i	2.58×10^{4}	0.53	0.24	111 i
CH_2O→CH_2+O	R16	0.22	−0.43	70 i	1.14×10^{12}	1.41	−0.16	374 i
CH_2O+H→CH_2OH	R17	1.16	0.78	1028 i	2.50×10^{2}	1.06	0.30	1195 i
CH_2O+H→CH_3O	R18	1.10	−0.38	600 i	2.11×10^{4}	0.65	−0.36	938 i
CH_3O→CH_3+O	R19	2.14	0.37	418 i	8.73×10^{-8}	1.53	−0.04	377 i
CH_3O+H→CH_3OH	R20	1.03	0.95	15 i	2.68×10^{4}	1.31	0.46	934 i
COH+H→HCOH	R21	0.87	0.46	260 i	9.30×10^{5}	0.95	0.72	252 i
COH→C+OH	R22	0.36	−0.60	306 i	9.78×10^{9}	2.01	0.66	232 i
OH→O+H	R23	0.91	0.11	1210 i	3.62×10^{3}	—	—	—

3.2.1 The initial CO activation

CO dissociation on La/Ni(111) only requires an E_a of 1.63 eV, which is much lower than the results of 3.74 eV on Ni(111) due to the incorporation of La into Ni. The catalytic activity of CO methanation on Ni catalyst is seen to have close relation with the activity to dissociate CO[27]. Again, the promoter La can promote HCO formation with an E_a reduced by 0.43 eV in comparison with Ni(111), while not facilitate the formation of COH, the adsorption of which have almost the similar structure characteristic with or without La. Although the E_a is as high as 2.11 eV for CO interaction with H to form COH formation, the dissociation of COH only needs to overcome as low as 0.36 eV. Given this, COH is also a possible product of CO activation.

3.2.2 All possible pathways for CH_4 formation

To comprehensively understand the mechanism of CO

methanation on La/Ni(111), taking all possible pathways involved in CO methanation is necessary. Based on the reaction network (Fig. 2), the potential energy diagrams of ten possible pathways leading to CH_4 on La/Ni(111) are summarized and presented in Fig. S4 in the Supplementary material.

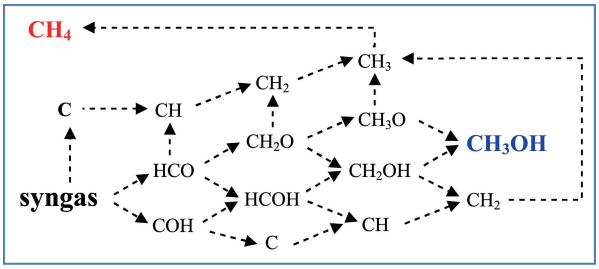

Fig. 2　Reaction network involved in CO methanation to form CH_4 and CH_3OH on La/Ni(111) surface

It is observed that the corresponding overall activation energies of ten pathways are 2.06, 2.04, 2.11, 2.07, 2.39, 2.41, 2.73, 2.77, 3.37, and 2.65 eV, respectively. For comparison, Path1, Path2, Path3, and Path4, corresponding to the lower overall activation energy of 2.06, 2.04, 2.11, and 2.07 eV, are identified as the energetically favorable pathways for CH_4 formation; the key intermediates of Path1, Path2, Path3, and Path4 are CO, HCO, COH, and CH_2O, correspondingly. And to be clear, there are two main strengths of Path1, Path2, Path3, and Path4, as expected: one is low energy barrier and the other is that no CH_3OH forms.

3.2.3　The energetically favorable pathways for CH_4 formation

As above, on La/Ni(111), Path1, Path2, Path3 and Path4, as presented in Fig. 3~6, are mainly responsible for CH_4 formation.

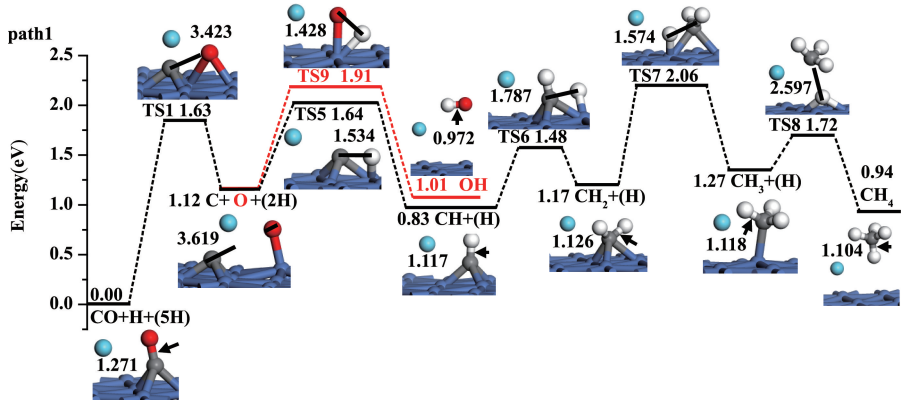

Fig. 3　The potential energy diagram of path1 together with the structures of the ISs, TSs and FSs involved in CO methanation to form CH_4 and OH on La/Ni(111) surface(The blue, gray, red, white and ultramarine balls represent Ni, C, O, H and La atoms, respectively; Bond lengths are in Å)

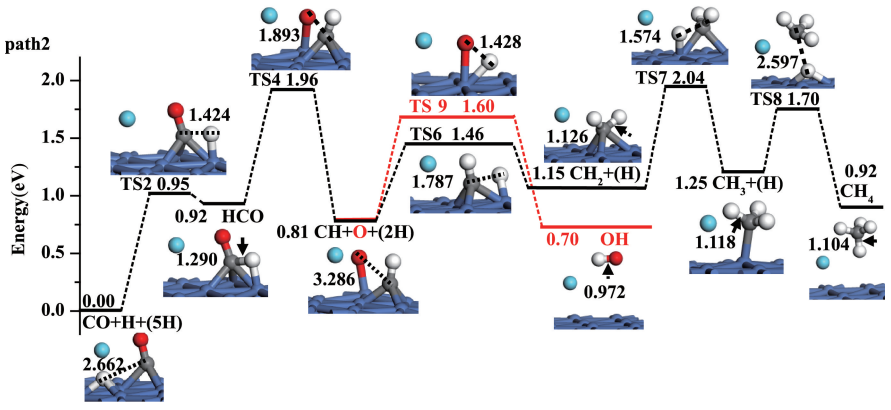

Fig. 4　The potential energy diagram of path2 together with the structures of the ISs, TSs and FSs involved in CO methanation to form CH_4 and OH on La/Ni(111) surface(Bond lengths are in Å, color coding see Fig. 3)

As shown in Path1 (see Fig. 3), the initial CO dissociation occurs on La/Ni(111). To produce CH_4 on La/Ni(111), the dissociated C then undergoes sequential hydrogenations to form CH_4. C hydrogenation to CH is exothermic with ΔE of

0.29 eV. The formations of CH_2 and CH_3 are thermodynamically uphill with 0.34 eV and 0.10 eV in ΔE, respectively; the formation of CH_4 is significantly exothermic by 0.33 eV. E_a for CH, CH_2, CH_3 and CH_4 formations are 0.52, 0.65, 0.89 and 0.45 eV, respectively; and the corresponding rate constants are 7.10×10^8, 2.57×10^7, 2.86×10^5 and 9.48×10^9 s^{-1} at 550 K, which are in accordance with earlier research (Table 2).

As shown in Path2 (see Fig. 4), the direct dissociation of HCO to CH and O is slightly exothermic by −0.11 eV, the corresponding E_a is 1.04 eV with the rate constant of 2.17×10^3 s^{-1}, which is much lower than the dissociation of CO (E_a = 1.63 eV) with the rate constant of 8.74×10^{-2} s^{-1}. Next, the produced CH is followed by the successive hydrogenations to CH_4.

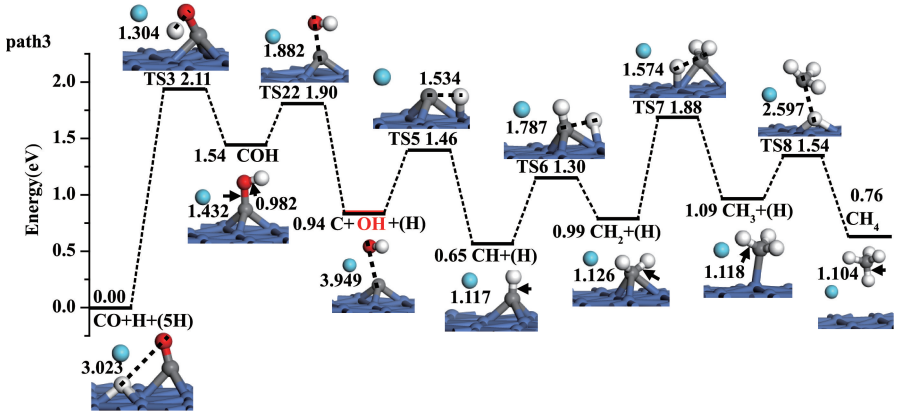

Fig. 5 The potential energy diagram of path3 together with the structures of the ISs, TSs and FSs involved in CO methanation to form CH_4 and OH on La/Ni(111) surface (Bond lengths are in Å, see Fig. 3 for color coding)

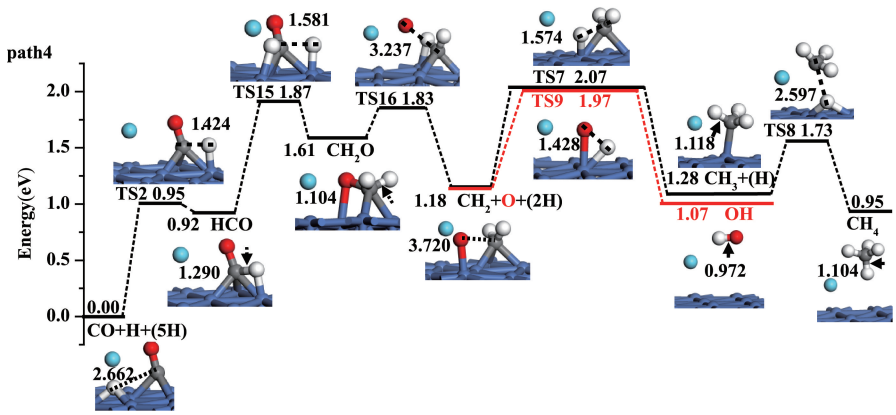

Fig. 6 The potential energy diagram of path4 together with the structures of the ISs, TSs and FSs involved in CO methanation to form CH_4 and OH on La/Ni(111) surface (Bond lengths are in Å, see Fig. 3 for color coding)

As shown in Path3 (see Fig. 5), COH dissociation is highly exothermic by 0.60 eV with an E_a of 0.36 eV, and this step has larger rate constant of 9.78×10^9 s^{-1}. Further, C undergoes four sequential hydrogenations to CH_4.

As shown in Path4 (see Fig. 6), the formation of CH_2O is thermodynamically uphill with 0.69 eV in ΔE, and the corresponding E_a is 0.95 eV with the rate constant of 2.58×10^4 s^{-1}. The produced CH_2O dissociates into CH_2 and O with an E_a of 0.22 eV; then CH_2 eventually leads to CH_4 formation.

In addition, the hydrogenation of the dissociated O is endothermic by 0.11 eV with an E_a of 0.91 eV, leading to the production of OH.

3.2.4 The effect of the by-product CH_3OH formation on the selectivity of CH_4 formation

During the generation of CH_4, the by-product CH_3OH can be formed by the hydrogenation of CH_2OH and/or CH_3O. As seen in Fig. S4 in the Supplementary material, Path7, Path8, Path9 and Path10 for the conversion of CO to CH_4 and

CH_3OH on La/Ni (111) share identical steps until the CH_2OH or CH_3O intermediates are formed. Herein, the selectivity of CH_4 and CH_3OH are controlled by the relative activity of CH_2OH or CH_3O hydrogenation and dissociation. It can be seen that most clearly, Path9 is kinetically feasible for CH_3OH formation with the overall activation energy of 2.71 eV, which is much higher than those of Path1, Path2, Path3 and Path4 (2.06, 2.04, 2.11 and 2.07) for CH_4 formation. This signifies that CH_3OH formation is inferior to CH_4 formation, and the preferred product from CO methanation on La/Ni(111) should be CH_4.

3.2.5 Microkinetic modeling

Although the DFT results obtained show that CH_4 formation is much more favorable than CH_3OH formation, it is incompletly only based on the overall activation energy and the rate constant. More precisely, at the experimental terms of $P_{CO}=25$ kPa, $P_{H_2}=75$ kPa and $T=550\sim750$ K[28-31], the rates of r_{CH_4} and r_{CH_3OH}, calculated using microkinetic modeling[32], can further be used to estimate the selectivity of CO methanation. The detailed calculations of r_{CH_4} and r_{CH_3OH} are presented in the Supplementary material. r_{CH_4} and r_{CH_3OH} are listed in Table 3, and the variation of the relative selectivity of $r_i/(r_{CH_4}+r_{CH_3OH})$ as a function of temperature is depicted in Fig. 7.

As depicted in Table 3, the rates r increase with the increasing of temperature on La/Ni(111), and r_{CH_4} is larger than r_{CH_3OH} at the same temperatures, suggesting that the productivity for CH_4 formation from syngas is higher than that for CH_3OH formation.

Table 3 The rates r (s^{-1} site^{-1}) for CH_4 and CH_3OH formations in CO methanation on La/Ni(111) surface at different temperatures

T/K	Rate/(s^{-1} site^{-1})	
	$r(CH_4)$	$r(CH_3OH)$
550	4.01×10^{6}	7.46×10^{-2}
575	1.04×10^{8}	4.40
600	2.05×10^{9}	1.82×10^{2}
625	3.15×10^{10}	5.59×10^{3}
650	3.94×10^{11}	1.32×10^{5}
675	4.10×10^{12}	2.45×10^{6}
700	3.61×10^{13}	3.67×10^{7}
725	2.75×10^{14}	4.41×10^{8}
750	1.83×10^{15}	4.07×10^{9}

As shown in Fig. 7, in $T=550\sim750$ K, the relative selectivity of CH_4 reaches almost as high as 100%[33], far above that of CH_3OH at the same temperatures, signifying that CH_3OH is hardly formed on La/Ni(111). The same is true in case that CH_4 selectivity increased to nearly 100% when La is added to Ni/γ-Al_2O_3 for CO_2 methanation[8,9]. Thus, the introducing La into Ni leads to a superior selectivity to CH_4 rather than CH_3OH. This agrees well with earlier researches[28,31], in which no CH_3OH is formed.

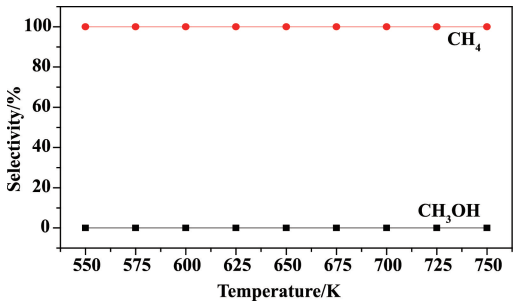

Fig. 7 The relative selectivities of the products CH_4 and CH_3OH on La/Ni(111) surface at the different temperatures using the microkinetic modeling

3.3 General discussions

3.3.1 Impact of the promoter La in La/Ni(111) on CO methanation

As schematically shown in Path1, Path2, Path3 and Path4 on La/Ni(111), the overall activation energies of 2.04, 2.07, 2.06 and 2.11 eV are favorable for CH_4 formation, which are reduced by up to 0.29 eV compared to earlier results of 2.33 eV[7] on Ni(111), indicating that a superior catalytic activity is observed over the modified La/Ni(111). The same is true in case that La increases the activity of Ni/γ-Al_2O_3 for CO_2 methanation[8,9].

In the case of the pure Ni(111), the formation of CH_4 from syngas is competitive with CH_3OH formation (2.33 *vs* 2.36 eV[7]). This is why the selectivity of Ni(111) for CH_4 formation needs to be improved by introducing La into Ni, and fortunately, this approach has turned out well. On La/Ni(111), in comparison with 2.71 eV for overall activation energy of CH_3OH by-product, CH_4 formation is much more favorable with a significant decrease of 0.67 eV due to the tuning effect of La, indicating that an excellent selectivity can be exhibited by the incorporation of La into Ni.

As stated above, introducing La into Ni performs the superior CH_4 activity and selectivity associated with the remarkable resistance to CH_3OH formation. This is indeed shown to be

the case in some other reports[34] that a CO conversion of almost 100% is obtained on La incorporated Ni-based methanation catalyst. Essentially, the rare earth element La is functioned as the electron modifier, which is helpful for activating CO molecule.

3.3.2 Electronic structure analysis based on the synergistic effect between La and Ni

As indicated by the results of DFT calculation and microkinetic modeling, introducing La into Ni can produce an excellent reactivity of CO methanation, and presumably as a result of the synergistic effect between La and Ni, which have been proven by the differential charge density of the La atom and Ni atoms on La surrounding surface over La/Ni(111) in Fig. 8.

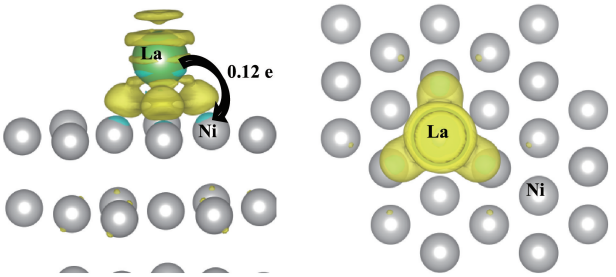

Fig. 8 The differential charge density of La atom and Ni atoms on La surrounding surface over La/Ni(111): (a) side view, (b) top view (The yellow and blue shaded regions represent charge loss and charge gain, respectively)

As can be seen from Fig. 8, charge loss behavior of La is happening in the yellow areas, while electron accepting behavior of Ni is occuring in the scattered blue areas. That is, there is depletion of electron density around the La atom and accumulation of electron density on the Ni atoms nearby the La atom. This "delocalization" allows electron transfer from the La atom to the electron-accepting Ni atoms placed nearby, suggesting that La makes its electrons available to the Ni atom over La/Ni(111). Thus far, the electron transfer occurs, La→Ni.

As presented in Fig. 9, it is the electron transfer from La to Ni that enriches d-band electron density of Ni atoms, leads to a shift of ε_d of La/Ni(111), and thereby improves the reactivity of Ni for CO methanation. This is known as the electron "delocalization effect"[35], partly as a result of the synergistic effect, the other result of which is the so-called structure "confinement effect", which leads to a decline in the crystallite size and a growth in the number of La/Ni reaction sites[8, 9, 11, 36], and ultimately creates a greater increase of the reactivity of CO

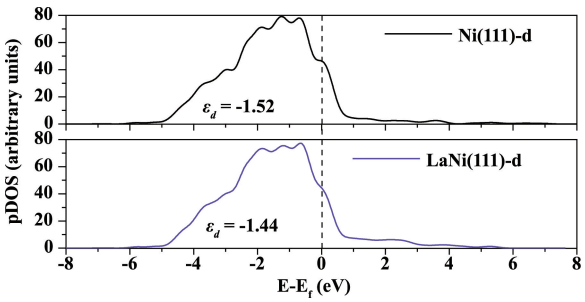

Fig. 9 Projected density of states pDOS for d-band center on Ni(111) and La/Ni(111) surfaces. The vertical black lines donate the Fermi level

methanation. Apparently, the addition of the promoter La remarkably modifies the electronic environment of the Ni(111).

3.3.3 Role of promoter La

Throughout the whole reaction network, compared to Ni(111), La/Ni(111) has exhibited a significant increase in reactivity of CO methanation. The main role of the promoter La is to weaken and then promote the cleavage of C—O bonds of CO, HCO, COH and CH_2O, which are respectively the key intermediates of Path1, Path2, Path3 and Path4 in CO methanation. This conclusion is further supported by Bader charges analysis[7, 19] and the projected density of states (pDOS)[26], which are depicted in Table 4 and Fig. 10, respectively.

For absorbed CO, HCO, COH and CH_2O, it can be clearly seen from Table 4 that the accumulation of charge is around the C atom when La is doped. The more charge number the C atoms (2.88, 3.03, 3.76 and 3.61 e) on La/Ni(111) carries, the less C positive electricity is, compared to those (2.52, 2.96, 3.29 and 3.12 e) on Ni(111), then it offers the weaker polar C—O linkage, and ultimately introduces the lower activation energy for C—O bonds breaking.

Besides, taking d_{C-O} of CO, HCO, COH and CH_2O on Ni(111) as the reference, the C—O bonds of CO, HCO, COH and CH_2O on La/Ni(111) are elongated, and the O atoms of CO, HCO, COH and CH_2O move towards the La due to the weakened C—O bonds, as seen from Table 4. This agrees with the calculated activation energy for breaking C—O bonds of CO, HCO, COH and CH_2O, as summarized in Table 2. Clearly, as d_{C-O} stretched, the activation energies of 1.63, 1.04, 0.36 and 0.22 eV corresponding to the C—O bonds cleavage of CO, HCO, COH and CH_2O gradually decrease, then until CH_2O has a minimum at a much longer C—O distance d_{C-O} = 1.432Å, that means the C—O bonds cleavage of CO, HCO, COH and CH_2O are much favorable when La is doped.

Table 4　Charges q of C and O atoms of CO, HCO, COH, and CH_2O as well as the promoter La and its nearest Ni atoms of La/Ni(111) and Ni(111) surfaces

Species	Charges, q/e			
CO	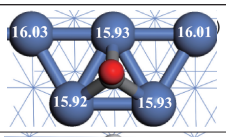	C : 2.52 O : 7.84 d_{C-O} = 1.194	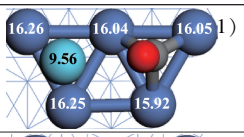	C : 2.88 O : 7.92 d_{C-O} = 1.271
HCO	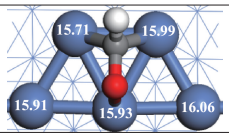	C : 2.96 O : 7.60 d_{C-O} = 1.294	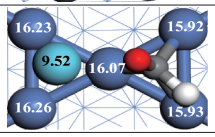	C : 3.03 O : 7.82 d_{C-O} = 1.319
COH	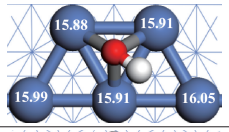	C : 3.29 O : 8.00 d_{C-O} = 1.337	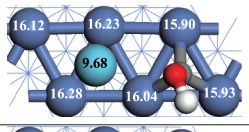	C : 3.76 O : 7.87 d_{C-O} = 1.399
CH_2O	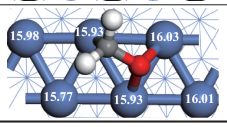	C : 3.12 O : 7.59 d_{C-O} = 1.385	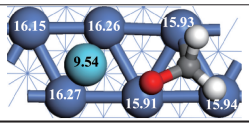	C : 3.61 O : 7.45 d_{C-O} = 1.432

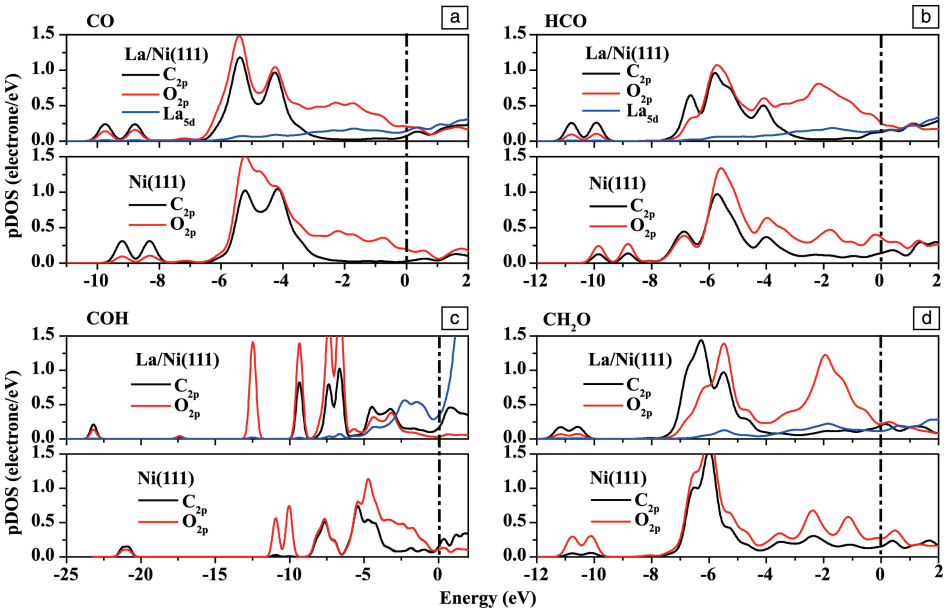

Fig. 10　Projected density of states (pDOS) for CO (a), HCO (b), COH (c) and CH_2O (d) chemisorptions on La/Ni(111) and Ni (111) surfaces. The vertical line indicates the Fermi level

As plotted in Fig. 10, on La/Ni(111), there are the hybridizations between C_{2p}, O_{2p} and La_{5d} orbitals, and note that the bonding states of C—O bonds of CO, HCO, COH and CH_2O, located below the E_f, move away the E_f relative to those on Ni(111). This is caused by electron donation from La to these molecules, similarly to which found for Cu cluster[37]. Namely, the C_{2p}—O_{2p} states is pulled below the E_f by the initial empty antibonding La_{5d}, which is partially filled due to La_{5d} participating in the charge transfer. Thus, the downshift of C_{2p}—O_{2p} states accelerates the C—O bonds cleavage of CO, HCO, COH and CH_2O.

As a consequence, the promoter La can weaken C—O bond strength, accelerate the cleavage of C—O bonds of CO, HCO, COH and CH_2O, and promote CO methanation; and the increase of the reactivity of CO methanation on La/Ni (111) can be ascribed to the introduction of the promoter La.

4　Conclusions

DFT results indicate that the enhanced catalytic activity of La/Ni(111) observed theoretically is the result of a decrease in the reaction barrier for C—O bond cleavage of CO、HCO、

CH_2O and COH, which are the key intermediates of Path1, Path2, Path3 and Path4 for CH_4 formation, respectively. On the other hand, the enhanced selectivity of La/Ni(111) compared to undoped Ni(111) in CO methanation is due to the lowering of the overall activation energy toward CH_4 formation and the significant increasing of that toward CH_3OH formation, and thereby leads to no CH_3OH yield.

Meanwhile, the results of the microkinetic modeling show that CH_4 selectivity is far above CH_3OH at any temperature between 550 K and 750 K, and CH_3OH is hardly formed on La/Ni(111). Moreover, the increase of CH_4 selectivity can be ascribed to introducting La into Ni, which have been proven by the differential charge density of the La atom and Ni atoms on La surrounding surface over La/Ni(111). The synergistic effect between La and Ni in La/Ni(111) displays significant effectiveness in maximizing CH_4 and minimizing CH_3OH.

Conclusively, the promoter La can weaken C—O bond strength, introduces the lower activation energy for C—O bonds breaking, and promote CO methanation. Namely, the superior activity and selectivity of La/Ni(111) is mainly originated from the synergistic effect between La and Ni.

Supplementary material: download link: http://www.mat-china.com/oa/DArticle.aspx?type=view&id=202009183

References

[1] LIU Q, GU F, LU X, *et al*. Applied Catalysis A: General[J], 2014, 488: 37-47.

[2] LIU Q, BIAN B, FAN J, *et al*. International Journal of Hydrogen Energy[J], 2018, 43(10): 4893-4901

[3] HUANG J, LI X, WANG X, *et al*. Journal of CO_2 Utilization[J], 2019, 33: 55-63.

[4] GAO J, JIA C, ZHANG M, *et al*. Catalysis Science & Technology[J], 2013, 3(8): 2009-2015.

[5] CATAPAN R, OLIVEIRA A A M, CHEN Y, *et al*. Journal of Physical Chemistry C[J], 2012, 116(38): 20281-20291.

[6] FANG X, XU L, ZHANG X, *et al*. Molecular Catalysis[J], 2019, 468: 130-138.

[7] ZHI C, WANG Q, WANG B, *et al*. RSC Advances[J], 2015, 5(82): 66742-66756.

[8] GARBARINO G, WANG C, CAVATTONI T, *et al*. Applied Catalysis B: Environmental[J], 2019, 248: 286-297.

[9] ARANDIYANA H, KASAEIAN G, NEMATOLLAHI B, *et al*. Catalysis Communications[J], 2018, 115: 40-44.

[10] TADA S, KIKUCHI R, TAKAGAKI A, *et al*. Catalysis Today[J], 2014, 232: 16-21.

[11] Gong D, Li S, Guo S, *et al*. Applied Surface Science[J], 2018, 434: 351-364.

[12] LU H, YANG X, GAO G, *et al*. Fuel[J], 2016, 183: 335-344.

[13] SI J, LIU G, LIU J, *et al*. RSC Advances[J], 2016, 6: 12699-12707.

[14] JIANG T, TIAN J, WANG N, *et al*. Acta Physico-Chimica Sinica[J], 2016, 32(10): 2531-2537.

[15] GOTO Y, MORIKAWA A, TANABE T, *et al*. ACS Applied Energy Materials[J], 2019, 2: 3179-3184.

[16] WANG W, ZHANG X, YANG Y, *et al*. Acta Physico-Chimica Sinica [J], 2012, 28: 1243-1251.

[17] MICHALSKA K, KOWALIK P, PRÓCHNIAK W, *et al*. Catalysis Letters[J], 2018, 148(3): 972-978.

[18] WIERZBICKI D, MOTAK M, GRZYBEK T, *et al*. Catalysis Today [J], 2017, 307: 205-211.

[19] ZHI C, ZHANG R, WANG B. Molecular Catalysis[J], 2017, 438: 1-14.

[20] LI J, CROISET E, RICARDEZ-SANDOVAL L. Journal of Catalysis [J], 2015, 326: 15-25.

[21] MITTENDORFER F, EICHLER A, HAFNER J. Surface Science[J], 1999, 423(1): 1-11.

[22] MORTENSEN J J, HANSEN L B, JACOBSEN K W. Physical Review B[J], 2005, 71: 035109-1-11.

[23] METHFESSEL M, PAXTON A T. Physical Review B[J], 1989, 40: 3616-3621.

[24] SHEPPARD D, TERRELL R, HENKELMAN G. Journal of Chemical Physics[J], 2008, 128(13): 134106-1-10.

[25] KAPUR N, HYUN J, SHAN B, *et al*. Journal of Physical Chemistry C [J], 2010, 114(22): 10171-10182.

[26] LI J, CROISET E, RICARDEZ-SANDOVAL L. Journal of Physical Chemistry C[J], 2013, 117(33): 16907-16920.

[27] LEE G D, MOON M J, PARK J H, *et al*. Korean Journal of Chemical Engineering[J], 2005, 22(4): 541-546.

[28] HE Z, WANG X, GAO S, *et al*. Applied Petrochemical Research[J], 2015, 5: 413-417.

[29] LIU Q, ZHONG Z, GU F, *et al*. Journal of Catalysis[J], 2016, 337: 221-232.

[30] LIU Q, GAO J, GU F, *et al*. Journal of Catalysis[J], 2015, 326: 127-138.

[31] MENG F, LI X, LI M, *et al*. Chemical Engineering Journal[J], 2017, 313: 1548-1555.

[32] ANDERSSON M P, ABILD-PEDERSEN F, REMEDIAKIS I N, *et al*. Journal of Catalysis[J], 2008, 255(1): 6-19.

[33] QIN H, GUO C, WU Y, *et al*. Korean Journal of Chemical Engineering[J], 2014, 31: 1168-1173.

[34] HAN Y, WEN B, ZHU M, *et al*. Journal of Rare Earths[J], 2018, 36 (4): 367-373.

[35] XU L, WANG F, CHEN M, *et al*. International Journal of Hydrogen Energy[J], 2017, 42(23): 15523-15539.

[36] ZHANG L, BIAN L, ZHU Z, *et al*. International Journal of Hydrogen Energy[J], 2018, 43(4): 2197-2206.

[37] DUAN Y, ZHANG J, FAN X, *et al*. Physica E[J], 2015, 73: 89-95.

(编辑 张雨明)